Innovative Food Science and Emerging Technologies 38 (2016) 124–130

Contents lists available at ScienceDirect

Innovative Food Science and Emerging Technologies

journal homepage: www.elsevier.com/locate/ifset

Morphological changes in multilayer polymeric films induced after microwave-assisted pasteurization

Kanishka Bhunia [a], Hongchao Zhang [a], Frank Liu [a], Barbara Rasco [b], Juming Tang [a], Shyam S. Sablani [a,*]

[a] Department of Biological Systems Engineering, Washington State University, P. O. Box-646120, Pullman, WA 99164-6120, United States
[b] School of Food Science, Washington State University, P.O Box 646376, Pullman, WA 99164-6376, United States

ARTICLE INFO

Article history:
Received 15 February 2016
Received in revised form 6 July 2016
Accepted 21 September 2016
Available online 22 September 2016

Keywords:
Dielectric properties
Gas barrier
Nylon
Pet
X-ray diffraction

ABSTRACT

In-package pasteurization of ready-to-eat (RTE) meals using microwave-assisted pasteurization system (MAPS) has shown promise for improving the safety and quality of foods, since dielectric heating is more efficient than thermal conduction. However, MAPS can affect the oxygen transmission rate (OTR) and water vapor transmission rates (WVTR) of packaging, imparting a certain degree of quality deterioration to the pasteurized food. This study evaluates morphological changes in newly-developed 3 multilayer polymeric films used for lid-stock on trays subjected to MAPS. We measured changes in OTR and WVTR after MAPS treatment, and further correlated these measurements with melting enthalpy (ΔH), overall crystallinity, crystal structure, water absorption, and dielectric properties of films. The composition of tested films was: (Film A): polyethylene terephthalate (PET)/barrier PET/polyethylene (PE); (Film B): PET/Nylon-Polypropylene (PP) and (Film C): PET/low density polyethylene (LDPE)/Nylon/LDPE. Results show that the OTR and WVTR of the films significantly increased ($P < 0.05$) after both hot water and MAPS pasteurization. Films B and C exhibited a higher OTR after MAPS (52 mins) compared to hot water pasteurization (36 mins). The melting enthalpy (ΔH) of the films increased after pasteurization, and was correlated to the increase in overall crystallinity (1–4% increase) of the films. Increases in OTR and WVTR can be attributed to the fragmented crystal structures and smaller crystal size observed in *X*-ray diffraction. It is evident that the films absorbed water during MAPS, which altered their dielectric properties. In addition, it is likely that water absorption caused plasticization of the Nylon polymer, degrading the gas barrier properties of the film. Based on these findings, we recommend using a multilayer film with PET as barrier layer for MAPS treatment.

Industrial relevance: Commercialization of novel microwave-assisted thermal pasteurization technology will require development of multilayer films which can sustain microwave and thermal stresses. Food processes influence oxygen and water vapor barrier properties of films which may affect the shelf-life of food sensitive to oxygen and water vapor. A better understanding of the influence of microwave-assisted thermal pasteurization process on film properties will help polymer industry in the design and development of improved film structures.

1. Introduction

Pasteurization involves processing foods at temperatures of 70 to 90 °C to inactivate vegetative bacterial cells and viruses of public health significance (Peng, Tang, Barrett, Sablani, & Powers, 2014). Thermally pasteurized food retains higher sensory and nutritional quality compared to sterilized foods. Pasteurized foods have a shelf life of several days to few weeks at refrigerated temperature. Conventional hot water and steam-based thermal processes result in a certain degree of quality degradation for prepared meals. Microwave heating has the potential to deliver superior quality processed food. This is because volumetric heating works more efficiently. The microwave-assisted thermal pasteurization system (MAPS), based on a single mode 915 MHz with surface water heating, was developed at Washington State University to produce pre-packaged high quality refrigerated food (Tang, 2015).

MAPS requires in-package food and the packaging must be transparent to microwave radiation. Metal-based packaging is not suitable, since it blocks microwave radiation. Although polymeric-based packaging is suitable for MAPS, the packaging must maintain its visual appearance and integrity after processing. Little research has examined the influence of thermal pasteurization (Halim, Pascall, Lee, & Finnigan, 2009), microwave- assisted thermal sterilization (MATS) (Dhawan et al., 2014a; Mokwena, Tang, Dunne, Yang, & Chow, 2009), or pressure-assisted thermal sterilization (PATS) (Dhawan et al., 2014b) on the barrier properties of polymeric films. Dhawan et al. (2014a) reported a reduction in gas barrier properties of PET-based multilayer films. They demonstrated that retort sterilization had more influence compared to MATS processing due to longer processing times associated with retort

* Corresponding author.
E-mail address: ssablani@wsu.edu (S.S. Sablani).

http://dx.doi.org/10.1016/j.ifset.2016.09.024
1466-8564/

processing. They correlated an increase in oxygen transmission rate with changes in crystallinity and free volume properties of the polymeric films. Mokwena et al. (2009) also reported that retort sterilization had more effect on the gas barrier properties of EVOH-based multilayer polymeric films than MATS processing. Deterioration in gas-barrier properties was attributed to the plasticization of the hydrophilic EVOH layer. Changes in gas barrier properties were often related to alteration in morphology of films; specifically, the crystalline structure, the proportion of crystalline and amorphous phase in the polymer, and free volume. Changes in oxygen and water vapor transmission rates were also related to melting enthalpy, and the melting peak of crystalline structure of semi-crystalline polymer using differential scanning calorimetry (DSC) (Halim et al., 2009; Kong & Hay, 2003). *X*-ray diffraction can further explain the morphological changes by calculating crystalline percentage in polymers (Yoo, Lee, Holloman, & Pascall, 2009). The higher the crystalline percentage, the greater the gas barrier properties and mechanical strength of polymeric films.

An understanding of morphological and gas barrier properties changes is required to design and develop multilayer film for microwave-assisted pasteurization process. This is the first study to determine changes in the morphology and barrier properties of multilayer films after microwave-assisted pasteurization treatment. The objective of this study is to investigate the influence of MAPS on gas barrier properties of three multilayer polymeric films. This study also examines post-pasteurization changes in terms of crystalline percentage, thermal and dielectric properties of polymeric packaging films and correlated to gas barrier properties.

2. Materials and methods

2.1. Multilayer polymeric films and rigid trays

Three multilayer polymeric films (A, B, and C) were selected as the lid film for this study. Film A had a structure of barrier layer of polyethylene terephthalate (PET), sandwiched between an outer layer of PET and an inner sealant layer of linear low density polyethylene (LLDPE), denoted as PET/barrier PET/tie/PE, with overall thickness of 88 μm. Film B consisted of an outer layer of PET and an inner layer of nylon 6 and polypropylene (PP) blend (PET/tie/Nylon 6-PP), with a total thickness of 104 μm. Film C was a coextruded structure with an outer layer of PET, a barrier layer of nylon 66, and an inner sealant layer of LDPE, denoted as PET/LLDPE/LDPE/tie/Nylon 66/tie/LLDPE/LDPE (thickness = 105 μm).

Rigid polymeric trays with a 10.5 oz (300 g) capacity (Silgan Plastics, Chesterfield, MO, U.S.A.) were selected for the packaging containers. The tray had the following structure: PP/regrind/tie/EVOH/tie/regrind/PP with total wall thickness of 1.1 mm, with an inner dimension of 14.0 cm × 9.5 cm × 3.0 cm.

2.2. Preparation of mashed potato

Mashed potato was prepared by mixing 15% (w/w) potato flakes (Oregon Potato Company, Pasco, WA) with preheated 84.5% (w/w) de-ionized water (80 ± 1 °C) and 0.5% (w/w) salt (Mokwena et al., 2009). The mixture was then cooled to ambient temperature (23 °C). Approximately 290 ± 1 g of mashed potato was filled into the rigid trays. The trays were then vacuum-sealed (400 mbar) with lid films (sealing conditions: 185 °C for 4 s dwell time) with a vacuum sealer (MULTIVAC T-200, Multivac Inc., Kansas City, MO, U.S.A.).

2.3. MAPS and hot water pasteurization processes

Pasteurization was carried out in a pilot scale 915-MHz, single mode, semi-continuous microwave assisted pasteurization system (MAPS) developed at Washington State University, Pullman, Washington. The system has four sections to simulate industrial processes, namely, preheating, MW heating, holding, and cooling. All sections were filled with water at controlled temperatures. A rigid metal carrier frame with a microwave transparent mesh was used to hold and transport the sealed trays through the cavities. The trays were loaded at the preheating section, which was maintained at 61 °C by hot water. The preheating section helps food to achieve a uniform initial temperature. After preheating, the trays were navigated through MW heating cavity. There, the foods were heated by MW energy and hot water maintained at 93 °C. The MW heating was followed by hot water heating (holding section) for product to reach 90 °C. Finally, all trays were cooled in the cooling section using tap water (23 °C). The process was designed to achieve a desired pasteurization value ($P^{7}_{90^{\circ}C} = 10$ min) for a 6 log reduction of psychrotrophic non-proteolytic *Clostridium botulinum* type E (ECFF, 2006) at cold spot in mashed potato. The time-temperature data of the cold spot of the trays were obtained using Ellab sensors (Ellab, Centennial, CO). Typical MAPS treatment of mashed potato involved preheating trays up to the temperature 61 °C for 30 mins, heating in the microwave section for 2 mins, hot water heating at 93 °C for 20 mins, followed by cooling for 5 min (Fig. 1). Thus, the overall processing time for MAPS would be 52 min (only heating time considered).

For conventional hot water pasteurization, the sealed trays were immersed in hot water in a steam-jacketed kettle, and the water temperature was maintained at 93 °C. The temperature of the cold spot was monitored by a T-type thermocouple (TMQSS-032U-6, 0.032-in. outer diameter, 6-in.-long, Omega Engineering, Stamford, Connecticut, U.S.A.). The time-temperature data (n = 2) were recorded at the cold spot in the mashed potato by a mobile data logger system (USB-TC, Measurement Computing, Norton, Massachusetts, U.S.A.).

The pasteurization value for both MAPS and hot water pasteurization was calculated using the general formula (Eq. (1)):

$$P^{z}_{T_{ref}} = \int_0^t 10^{(T(t)-T_{ref})/z} dt \quad (1)$$

where $T(t)$ is the temperature of the cold spot, T_{ref} is the reference temperature, and the z value of the psychrotrophic non-proteolytic C. *botulinum* is 7 °C (ECFF, 2006). The overall exposure time for conventional hot water pasteurization to achieve $P^{7}_{90^{\circ}C} = 10$ min was approximately 36 min for all trays studied (Fig. 1). After pasteurization, the trays were rapidly cooled using tap water (23 °C). The lid films were carefully peeled from trays, wiped with dry paper and stored in glass vessels at room temperature (23 °C).

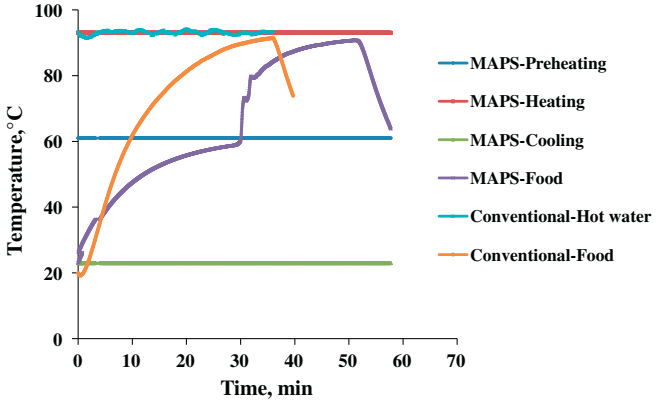

Fig. 1. Time-temperature profile of slowest heating region inside packaged mashed potato in a 10-oz tray during pasteurization.

2.4. Water content

The amount of water content in the film samples were measured gravimetrically. Approximately 0.1 ± 0.02 g of sample was taken in an aluminum pan and dried in a vacuum oven set at 25 in. vacuum and 70 °C for 2 days. The moisture content (% dry basis) was calculated as follows (Eq. (2)):

$$\text{Water content } (\%db) = \frac{M_t - M_d}{M_d} \times 100 \quad (2)$$

where M_t and M_d is the weight of the treated or control sample and dried sample in g, respectively.

2.5. Gas barrier properties

2.5.1. Oxygen transmission rate

Oxygen transmission rates (OTRs) of the film samples were measured using Ox-Tran 2/21permeability instrument (Mocon, Minneapolis, MN, U.S.A.) at 23 °C and 55 ± 1% relative humidity, 1 atm, according to the ASTM standard D3985 method (ASTM, 2010). A specially shaped die was used to cut film specimens with a 50 cm^2 surface area, which were mounted inside the testing chamber. The instrument was equipped with a Coulox oxygen sensor that reacts with transmitted oxygen and produces an electrical current that is proportional to the amount of oxygen entering the sensor. The control (untreated) and pasteurized lid films were measured in triplicate.

2.5.2. Water vapor transmission rate

A Mocon Permatran 3/33 instrument (Mocon, Minneapolis, MN, U.S.A.) was used to conduct water vapor transmission rate (WVTR) measurement of the lid films. The test conditions were set at 37.8 °C, 100% RH (ASTM standard method F1249-13) (ASTM, 2013). Similar to the OTR measurement, film specimens of 50 cm^2 surface area were cut and placed inside the testing chambers. An inbuilt infrared photo detector senses the change in energy due to the absorption rate of infrared energy by water vapor, and produces an electrical signal that is proportional to the water vapor transmission rate of the film specimen. The control and processed lid films were measured in triplicate.

2.6. Thermal analysis

A modulated differential scanning calorimetry (MDSC, model Q2000, TA instruments, New Castle, DE, U.S.A.) was used to study the change in initial crystallinity of the films. MDSC has advantages over DSC to characterize the overlapping transitions of endothermic (melting) and exothermic events (cold crystallization) in a multicomponent material (Verdonck, Schaap, & Thomas, 1999). In MDSC, a typical underlying heating rate of 1–5 °C is applied for polymers to allow sufficient modulation during heating (TA-211B, 2016; Solarski, Ferreira, & Devaux, 2005). About 9.0 ± 0.5 mg of film samples were sealed in an aluminum pan and placed in a DSC furnace. The sample was heated from 20 °C to 300 °C at a heating rate of 1 °C/min with amplitude of ±0.16 °C every 60 s. The obtained thermograms were analyzed for the peak melting point (T_m, °C) and the enthalpy due to relative crystallinity (ΔH, J/g) using thermal analysis software (Universal Analysis, TA Instruments). The T_m was determined from the peak temperature of the melting endotherm. The relative crystallinity (ΔH) was calculated as follows (Eq. (3)):

$$\Delta H = \Delta H_m - \Delta H_c \quad (3)$$

The melting enthalpy due to relative crystallinity (ΔH) was calculated from the sum of all melting enthalpies (ΔH_m) and enthalpies due to cold crystallization and crystal perfection (ΔH_c) observed in the reversing and non-reversing component of the signal during the heating scan. All the measurements were taken in triplicate.

2.7. X-ray diffraction

X-ray diffractograms of all control (untreated) and pasteurized films were obtained using a Siemens D-5000 diffractometer (Bruker, Karlsruhe, Germany). The diffractometer operated at a wavelength of 0.15 nm, and the copper target tube was set at 35 KV and 30 mA. The intensity of diffraction was recorded as a function of the increasing scattering angle from 8 to 45°, with a step angle of 0.05° and a scan time of 3 s per step. The XRD patterns were analyzed for percentage overall crystallinity, *d*-spacing (Angstrom, Å), full width at half maximum (FWHM) and crystal size (Angstrom, Å) using Jade 6 software (Materials Data Inc., Livermore, CA). This method enhances our understanding on the structural changes in terms of crystallinity in order to correlate gas barrier changes in films after pasteurization processes. The peaks of the obtained diffractograms were fitted using pseudo-voigt shape function. The crystallinity percent in the polymers was calculated from the ratio between total area under crystalline peaks and total area under all peaks. From the peak intensities of the X-ray diffractogram, *d*-spacing between lattice planes can be obtained using Bragg's law (Eq. (4)):

$$n\lambda = 2d\sin\theta \quad (4)$$

where n is an integer; λ is the X-ray wavelength used for the study (1.54 Å); θ is the angle of incidence with lattice plane. The crystal size (D) was obtained using the Scherrer equation as follows (Eq. (5)):

$$D = \frac{K\lambda}{\beta\cos\theta} \quad (5)$$

where K is the Scherrer constant and the value was taken as 0.9, λ = 1.54 Å, β is the full width at half maximum, and θ is the angle between incident rays obtained from the XRD peaks.

2.8. Dielectric properties

The dielectric properties of film samples (control and treated) were measured by Split post dielectric resonator (SPDR) methods (Clarke, 2007). Sample specimens of dimensions of about 90 mm × 85 mm were cut from the lid films and carefully placed into the opening of the SPDR cavity. The SPDR system was set at operating frequency of 2.668 GHz and connected to a 2 port Network Analyzer (E5071C, ENA Series, Agilent Technologies, Santa Clara, CA, U.S.A.). Prior to the measurements the empty cavity was calibrated with air for the resonant frequency and quality factor. The dielectric loss (ε''), dielectric constant (ε'), and loss tangent ($\tan\delta = \varepsilon''/\varepsilon'$) of the film specimens were analyzed with software (85071E Material Measurement software). Measurements were conducted in triplicate.

2.9. Data analysis

The experimental data of gas barrier properties, melting enthalpy, dielectric properties, and moisture content of the films before and after pasteurization were analyzed using a completely randomized design (CRD). A general linear model with Fisher's Least Significant Difference (LSD) was employed to determine significant differences ($P < 0.05$) in the film properties. The obtained data were reported as mean values and standard deviation (SD) from the result of three replicates. A commercial statistical software SAS version 9.2 (SAS Inst. Inc., Cary, NC, U.S.A.) was used to conduct the data analysis.

3. Results and discussion

3.1. Oxygen transmission rate

The OTRs of control films A, B, and C were 0.7, 0.1, and 2.3 cm^3/m^2-day at 55 ± 1% RH and 23 °C, respectively. Film B had the highest barrier property, followed by film A and then film C. Although all three films maintained visual appearance and integrity, the OTR values of films A, B and C increased to 1.5, 1.1, and 6.0 cm^3/m^2-day after hot water pasteurization and 1.1, 1.7, and 7.9 cm^3/m^2-day after MAPS (Fig. 2). Thus, there was a 114% and 57% increase in the OTR of film A after hot water pasteurization and MAPS, respectively. At the same time, the OTR of the film B increased by 1000% after hot water pasteurization and 1600% after MAPS. For film C, those values were 161% and 243% after hot water and MAPS treatment, respectively. Thus, both processes significantly increased ($P < 0.05$) the OTRs of the films.

Both structure of the films and process time influenced the changes in OTR. Since film B and C has hydrophilic nylon in their structure, a fractional increase in free volume due to plasticization can be expected more in comparison to film A. Film B contained nylon 6 in its sealing layer whereas Film C had nylon 66, protected by PET and LDPE from both sides. Therefore, nylon 66 in film C tends to absorb less moisture compared to the nylon 6 in film B because of its reduced polarity and protection from outer environment. Film A has hydrophobic PET as main barrier layer, and the increase in OTR after pasteurization can be considered as a net result of structural and morphological changes, rather than a plasticizing effect (Dhawan et al., 2014a). During pasteurization, films absorbed water, which acted as plasticizer. Absorbed water weakens the inter-chain hydrogen bonding in the amorphous phase of the polymer, and increases the chain mobility and fractional free volume (Lopez-Rubio et al., 2003). The increase in free volume could be one of the main reasons of increase in OTR of films (Dhawan et al., 2014b).

In addition to the structure of the film, the process time also influences the OTR of the films. The process time with MAPS was longer than hot water pasteurization. Plasticization of hydrophilic polymers by water absorption is a time-dependent process (Lopez-Rubio et al., 2003). Thus, longer processing time of MAPS (52 mins) might have led to greater reduction in oxygen barrier property of the films B and C compared to hot water pasteurization (36 mins).

Dhawan et al. (2014a) found that degradation in oxygen barrier property of PET based multilayer film was much higher after retort processing compared to MATS. Similar observations were also made by Mokwena et al. (2009), who investigated the effect of MATS and retort processing on hydrophilic EVOH films. Both studies attributed less change in oxygen barrier properties to the shorter processing time during MW (9 min) compared to retort (28 min) heating. However, in our study, overall processing time with MAPS was higher than that of conventional heating due to a longer preheating time. Halim et al. (2009) studied the influence of pasteurization (75 °C for 30 min), high-pressure processing (70 °C at 800 MPa for 10 min) and retort sterilization (121 °C for 30 min) on Nylon, Nylon/EVOH, and Nylon/Nanocomposite films. They also found that thermal pasteurization significantly decreased the barrier properties of nylon and nylon/nanocomposite films, with the exception of nylon/EVOH film.

3.2. Water vapor transmission rate

The WVTR of the films increased significantly ($P < 0.05$) after both hot water pasteurization and MAPS treatment (Fig. 3.). However, the level of increase in WVTR of the films after hot water pasteurization (13–46%) and MAPS (17–36%) treated films was similar. The changes in WVTR after hot water pasteurization and MAPS for film B (36 to 45%) were higher than films A (17–21%) and C (13–17%).

3.3. Thermal analysis

Table 1 shows the melting peaks (T_m) and enthalpy due to relative crystallinity (ΔH) of polymeric films before and after treatment. Pasteurization processes (hot water and MAPS) significantly increased ($P < 0.05$) the overall relative crystallinity (ΔH) of the film A compared to that of control films (Table 1). The relative crystallinity for film A increased after hot water pasteurization ($\Delta H = 23.0$ J/g) compared to the control ($\Delta H = 21.1$ J/g), and it is even higher for the MAPS process ($\Delta H = 24.5$ J/g). For film B, the overall relative crystallinity significantly increased ($P < 0.05$) after MAPS. The overall relative crystallinity of film C significantly decreased ($P < 0.05$) after hot water pasteurization ($\Delta H = 33.8$ J/g), but increased after MAPS ($\Delta H = 40.6$ J/g) compared to the control films ($\Delta H = 38.5$ J/g). It is important to note that the crystallinity of functional barrier layers in multilayer polymeric films contribute significantly to the gas barrier properties of the films. Thus, analysis of the relative crystallinity of individual layers is necessary. Below, we examined the relative crystallinity of individual layers and their plausible relation to the gas barrier properties of films after pasteurization processes. The typical melting thermogram for film B after pasteurization is shown in Fig. 4.

The functional barrier layers are PET in film A, PET and nylon in both films B and C. For control film A, peaks were observed at 124.3 °C (peak 1–PE layer), 170.5 °C (peak 2–tie layer), and 257.5 °C (peak 3–PET layer) (Table 1). The relative crystallinity values at corresponding melting

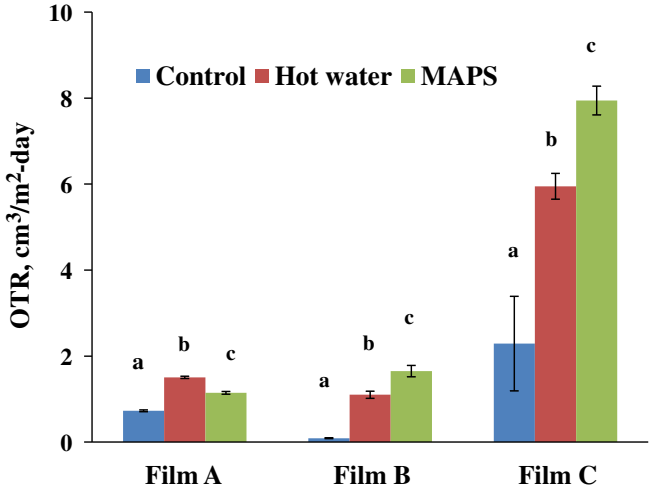

Fig. 2. Oxygen transmission rate of films before and after hot water pasteurization and MAPS.

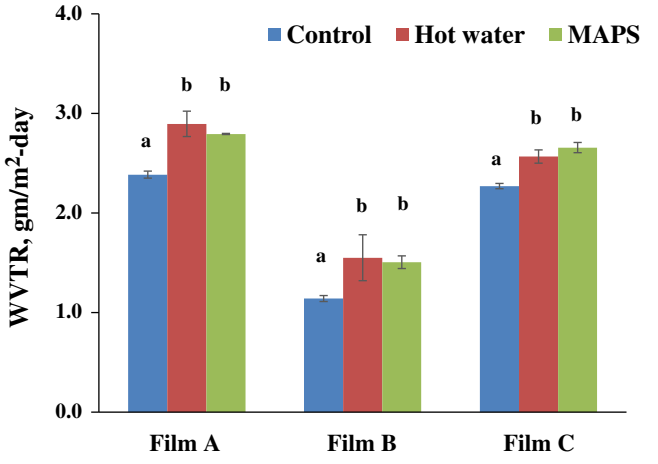

Fig. 3. Water vapor transmission rate of films as influenced by hot water pasteurization and MAPS.

Table 1
Melting temperature and enthalpy due to relative crystallinity of the individual layers in films before and after pasteurization processes.

Film	Treatment	Relative crystallinity (ΔH, J/g)	Relative crystallinity at peaks (ΔH, J/g)			Melting peak (T_m, °C)		
			Peak 1	Peak 2	Peak 3	Peak 1	Peak 2	Peak 3
A	Control	21.1 ± 0.4^{a}	11.0 ± 0.3^{a}	7.1 ± 0.1^{a}	3.1 ± 0.1^{a}	124.3 ± 0.2^{a}	170.5 ± 1.5^{a}	257.5 ± 0.7^{a}
	Thermal	23.0 ± 0.1^{b}	11.7 ± 0.1^{b}	6.4 ± 0.1^{b}	4.8 ± 0.1^{b}	124.0 ± 0.9^{a}	167.3 ± 0.5^{a}	256.1 ± 0.7^{a}
	MAPS	24.5 ± 0.3^{c}	11.9 ± 0.1^{b}	7.1 ± 0.1^{a}	5.5 ± 0.3^{c}	123.1 ± 0.1^{a}	167.7 ± 0.1^{a}	257.2 ± 0.7^{a}
B	Control	43.5 ± 0.7^{a}	22.3 ± 0.3^{a}	12.2 ± 0.4^{a}	9.0 ± 0.1^{a}	165.6 ± 0.1^{a}	221.2 ± 0.3^{ab}	257.0 ± 0.1^{a}
	Thermal	44.3 ± 0.4^{a}	23.6 ± 0.2^{c}	14.4 ± 0.1^{c}	6.4 ± 0.1^{c}	166.1 ± 0.7^{a}	220.6 ± 0.1^{a}	255.8 ± 0.3^{b}
	MAPS	46.3 ± 0.2^{b}	25.1 ± 0.2^{b}	13.5 ± 0.3^{b}	7.7 ± 0.1^{b}	166.0 ± 0.1^{a}	221.8 ± 0.2^{b}	256.2 ± 0.3^{ab}
C	Control	38.5 ± 0.5^{a}	29.7 ± 0.2^{a}	2.9 ± 0.3^{ab}	5.9 ± 0.4^{ab}	111.1 ± 0.1^{a}	169.5 ± 0.1^{a}	256.5 ± 0.2^{a}
	Thermal	33.8 ± 0.5^{b}	26.0 ± 0.1^{b}	2.1 ± 0.2^{a}	5.8 ± 0.3^{a}	111.4 ± 0.2^{a}	169.6 ± 0.6^{a}	258.7 ± 0.3^{b}
	MAPS	40.6 ± 0.1^{a}	28.1 ± 0.2^{a}	3.7 ± 0.5^{b}	6.8 ± 0.2^{b}	112.4 ± 0.9^{a}	169.3 ± 0.1^{a}	256.3 ± 0.2^{a}

Values are given as mean ± SD and compared along rows and columns; Values with different letters at superscript are significantly different ($P < 0.05$).

peaks were 11.0 (at peak 1), 7.1 (at peak 2), and 3.1 J/g (at peak 3). After pasteurization, the relative crystallinity corresponding to first two peaks remained almost unchanged, but increased to 4.8 and 5.5 J/g for peak 3 after hot water pasteurization and MAPS processes. Dhawan et al. (2014a) observed an increase in the melting enthalpy of the PET layer in multilayer polymeric films after MATS and retort processing. Film B also showed three melting peaks at 165.6 °C (PP), 221.2 °C (nylon), and 257.2 °C (PET). The ΔH for PET layer decreased after hot water pasteurization and MAPS but it increased for Nylon. The melting peaks of the film C were observed at 111.1 °C (LDPE), 169.5 °C (tie layer of maleic anhydride PE), and 256.5 °C (PET). Note that this study did not measure the melting peak for nylon. Nylon has wide range of melting points, from 220 °C (Nylon 6) to 265 °C (Nylon 66). It is possible that the melting peak of nylon is masked by the PET melting peak, since PET has a similar melting region. Another reason could be the low amount of nylon used in the film. Yeh, Yao, Du, and Chen (2005) did not observe any EVOH melting peaks in DSC thermograms of a modified polymer resin containing EVOH of 33.3% and lower. The ΔH for PET layer did not show any significant differences after hot water pasteurization compared to the control, but it increased somewhat after MAPS (5.9 to 6.8 J/g). Overall, results from MDSC for the studied polymers may be helpful in explaining the improvement of crystalline structures after both hot water and MW processing, but these results didn't correlate with post processing changes in the gas barrier of films. MDSC results were further correlated to the total crystallinity of the polymer obtained from the *X*-ray diffraction study.

3.4. X-ray diffraction

The *X*-ray diffraction patterns for film A before and after treatments are presented in Fig. 5. The major peaks observed nearly at $2\theta = 21.6$ and 26° corresponded to PE and PET (Dhawan et al., 2014a), respectively. The peak intensity at 21.6° was found to be higher for control film A than for the other two films. At $2\theta = 26°$ (PET crystalline structure), the peak intensity increased after hot water pasteurization, but somewhat decreased after MAPS. However, the overall crystallinity increased after both hot water pasteurization (53%) and MAPS (52%) compared to the control film (49%) (Table 2). Such an increase in PET crystallinity can be attributed to a process called 'chemicrsytallization' (Sammon, Yarwood, & Everall, 2000). Chemicrystallization is the result of hydrolytic degradation of PET polymer at temperatures above the glass transition (65–75 °C). During this process, the amorphous region undergoes chain scission to produce smaller chain fragments with enhanced mobility, which aids crystallization. The increase in crystallinity improves the barrier properties of the film. Although the crystallinity of the polymer structure was found to be higher after pasteurization, a wider peak (FWHM value from 1.203 to 1.269) occurred at 26° (PET structure) (data not shown). The associated decrease in crystal size (69 Å to 65 Å) indicates a disrupted crystal structure due to crystal fractionation (López-Rubio et al., 2005). The distorted crystal structures observed here could be one of the main reasons for decreased barrier performance.

Fig. 6 illustrates the diffraction pattern of film B as influenced by hot water pasteurization and MAPS. Three crystalline peaks, below $2\theta = 20°$ (PP crystalline structure) and two peaks nearly at 24° (nylon) and 26° (PET crystalline structure) were observed. There was an increase in peak intensities after MAPS, leading to an increase in crystallinity of MAPS-treated film (58% to 60%) (Table 2). An increase in peak intensities was observed at $2\theta = 24°$ (Nylon layer) and $2\theta = 17°$, 18.7°, and 14.2° (PP layer), indicating an improvement in the crystalline morphology of films. On the other hand, hot water pasteurization led to little decrease in peak intensities (Fig. 6), with a decrease in crystallinity to 55%.

Fig. 7 shows the diffraction pattern of film C after hot water and MAPS treatment. Major peaks were observed nearly $2\theta = 21.6°$ and

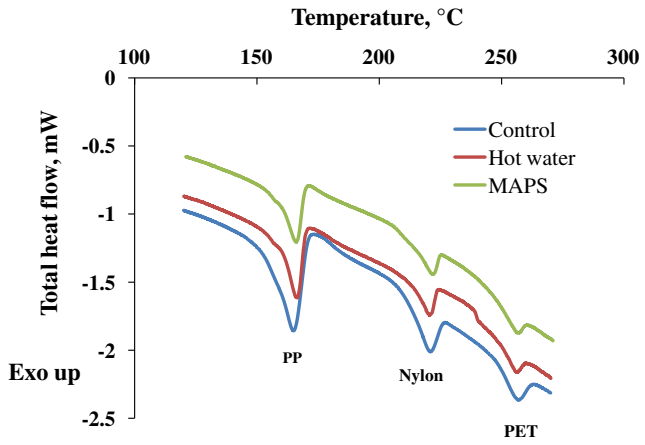

Fig. 4. Melting peaks of film B before after hot water pasteurization and MAPS.

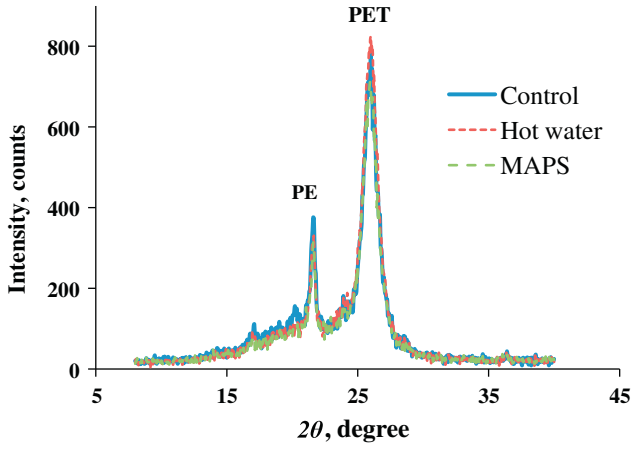

Fig. 5. X-ray diffraction patterns of film A before and after pasteurization processes.

Table 2
Overall crystallinity of films before and after hot water pasteurization and MAPS as determined by XRD.

Film	Treatment	Overall crystallinity (%)
A	Control	49
	Hot water	53
	MAPS	52
B	Control	58
	Hot water	55
	MAPS	60
C	Control	50
	Hot water	51
	MAPS	54

26°, corresponding to the PE and PET layer. Two additional smaller peaks were also observed at $2\theta = 9.5°$ and 28.7°. However, major peaks for Nylon at $2\theta = 24$ and 20° (Rabiej, OstrowskaGumkowska, & Wlochowicz, 1997) was not clearly visible. There are almost no changes in intensities for all peaks (Fig. 7). Broadening of the peak was observed after both pasteurization processes at $2\theta = 26°$. However, the peak at $2\theta = 21.6°$ became wider after hot water pasteurization (FWHM value: 0.436 to 0.462; crystal size: 192 Å to 180 Å), whereas it became narrower after MAPS (FWHM value: 0.436 to 0.407; crystal size: 192 Å to 206 Å). These changes in crystalline structure might have resulted in improved crystallinity of MAPS treated film (50 to 54%). Almost no changes in crystallinity were observed after hot water pasteurization (50 to 51%). The overall crystallinity of the polymeric films and their changes after pasteurization also contributed by morphology of the adhesive or tie layers manufactured by different companies, further influencing the gas barrier properties of the films. Although the crystallinity of the films increased after the pasteurization processes, the fragmented crystal structure and reduction in crystal size may explain the increase in the OTR and WVTR of pasteurized films.

3.5. Influence of absorbed moisture on dielectric properties

An increase in moisture content was observed for both hot water and MAPS-treated films compared to control samples (Table 3). Films A, B, C had the initial moisture of 0.7, 1.9, and 1.3 (% db), respectively. The moisture content increased by 2.6, and 1.52 times for films A, B and C, respectively after hot water pasteurization. These were even higher for MAPS-treated samples: 3.1 times for Film A, 1.9 times for Film B, and 2.4 times for Film C. During MAPS processing, packaging remained above ambient temperature for a longer time (~52 min) than in conventional hot water pasteurization (~36 min). This can be attributed to higher moisture absorption by the films during MAPS process.

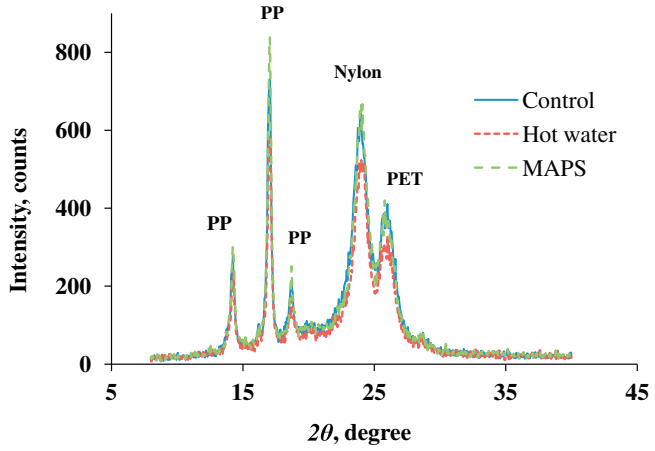

Fig. 6. X-ray diffraction patterns of film B as influenced by pasteurization processes.

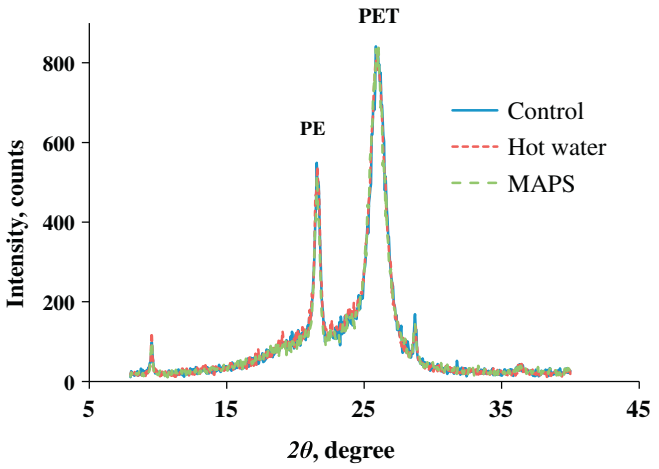

Fig. 7. X-ray diffraction patterns of film C before and after pasteurization treatments.

The dielectric constant (ε') of the films A, B and C was 2.46, 2.51, and 2.47, respectively (Table 3). Films with a low dielectric constant and loss are suitable for microwave processing. Results show that ε' decreased after hot water pasteurization for film A (2.46 to 2.40) but remained constant after MAPS processing for all films. However, no significant ($P > 0.05$) differences in ε' were found between the two pasteurization processes.

The measured value of the dielectric loss ($\varepsilon'' = \varepsilon' \tan\delta$) of films A, B, and C was 0.018, 0.013, and 0.010, respectively. The initial loss value of film A was higher, followed by films B and C. The barrier polymer of film A is PET, which is relatively less polar than nylon (one of the functional barrier layer in films B and C). However, the molar percentage of the polar group also contributes to dielectric loss of polymer films (Chen, Siochi, Ward, & McGrath, 1993). Film A contains higher fraction of PET (skin and barrier layer of PET), whereas films B and C has less fraction of nylon (only barrier layer) in their multilayer structures. The loss value increased to 0.019, 0.018, and 0.013 after hot water pasteurization and 0.020, 0.024, and 0.017 after MAPS processing. Dielectric loss (ε'') of films was higher after MAPS processing than hot water processing (Fig. 8). This can be explained by a higher water uptake by MAPS-treated films (Table 3).

Pasteurization resulted in an increase in ε''s by 1–1.1 times for film A, followed by film B (1.4–1.8 times) and Film C (1.3–1.7 times). Film B and C showed more change in ε''s and tan δ than film A. Film A absorbed a significant amount of water, but the influence of absorbed water was not reflected on the loss properties of film A, unlike films B and C. This can be explained by the dipole moment of the functional group of nylon (3–4 Debye for amide group), which is higher than PET (1–2 Debye for ester group). However, unlike PET, the absorbed water in nylon-containing polymers can form inter-molecular and intra-molecular hydrogen bonding, which is one of the most important factor in determining dielectric properties of the film (Chen et al., 1993). In a study with PET, ε'' and tan δ were greater for amorphous PET compared to crystalline PET, and the loss increased for wet samples (Reddish, 1950). The terminal —OH group in the crystalline PET did not contribute to the associated loss, due to the hindered movement —OH group and the different relaxation behavior in the crystalline region (Reddish, 1950). The dielectric properties of the polymers is highly dependent on the type of functional group, group dipole moments, mole percentage of polar groups, hydrogen bonding, percentage crystallinity, and physical state of polymers (Chen et al., 1993). The values of tan δ of processed and control films were found to be within the range of 0.004–0.009, which indicates that the films are low-loss materials.

As previously noted, this was the first study evaluating the changes in barrier properties of 3 multilayer films treated in newly developed MAPS. The MAPS process used low microwave power (4 kW), 30 mins

Table 3
Moisture content and dielectric properties of films after pasteurization processes.

Film	Treatment	Moisture content, % db	Dielectric constant, ε′	Dielectric loss, ε″	Loss tangent tan δ
A	Control	0.7 ± 0.3[a]	2.46 ± 0.04[a]	0.018 ± 0.001[a]	0.007 ± 0.001[a]
	Hot water	1.8 ± 0.5[b]	2.40 ± 0.03[b]	0.019 ± 0.001[a]	0.007 ± 0.001[a]
	MAPS	2.2 ± 0.4[b]	2.45 ± 0.02[ab]	0.020 ± 0.002[b]	0.008 ± 0.001[b]
B	Control	1.9 ± 0.5[a]	2.51 ± 0.04[a]	0.013 ± 0.001[a]	0.005 ± 0.002[a]
	Hot water	2.9 ± 0.6[b]	2.48 ± 0.03[a]	0.018 ± 0.001[b]	0.007 ± 0.002[b]
	MAPS	3.7 ± 0.5[b]	2.53 ± 0.03[a]	0.024 ± 0.001[c]	0.009 ± 0.001[c]
C	Control	1.3 ± 0.2[a]	2.47 ± 0.04[a]	0.010 ± 0.001[a]	0.004 ± 0.002[a]
	Hot water	2.0 ± 0.2[b]	2.41 ± 0.01[a]	0.013 ± 0.002[b]	0.005 ± 0.001[a]
	MAPS	3.1 ± 0.3[c]	2.46 ± 0.03[a]	0.017 ± 0.002[c]	0.007 ± 0.001[b]

Values are given as mean ± SD and compared along rows and columns; Values with different letters at superscript are significantly different ($P < 0.05$).

of preheating in 61 °C water, and 20 mins exposure to 93 °C circulating water. This resulted in longer processing time than conventional hot water treatment for a similar pasteurization value. Results highlight the need to improve current MAPS processing schedules to improve packaging performance. Our research team is now developing better process schedules by increasing microwave power, reducing exposure time in preheating, heating and holding zones. This may yield a net improvement of food quality and less damage to packaging films. Further research on the performance of packaging films under different processing conditions of MAPS is needed.

4. Conclusions

This study found that both hot water and microwave-assisted thermal pasteurization caused a significant decrease ($P < 0.05$) in oxygen and water vapor barrier of the studied multilayer polymeric films. The level of reduction in barrier properties of film A was significantly higher after hot water pasteurization compared to MAPS. On the other hand, the deterioration level in films B and C was higher after MAPS compared to hot water pasteurization. Our study reveals that irrespective of pasteurization processes, increase in OTR in films B and C was higher compared to film A. Decrease in barrier properties of multilayer films depends on hydro-philic/phobic nature of polymeric layers, overall exposure time and temperature of pasteurization processes, plasticization of films due to absorbed moisture, decreased crystallinity, and distorted crystal structures. Our findings suggest that polymeric packaging films with PET as a barrier layer may be appropriate for processing of ready-to-eat (RTE) foods using MAPS.

Acknowledgements

This work was partially funded by a USDA-NIFA Food Safety Grant #2011-68003-20096. The authors would like to thank Bemis-Curwood, Neenah, Wisconsin, Cryovac-Sealed Air, NJ, and Shields Bag and Printing, Yakima, WA for fabricating multilayer films for this study.

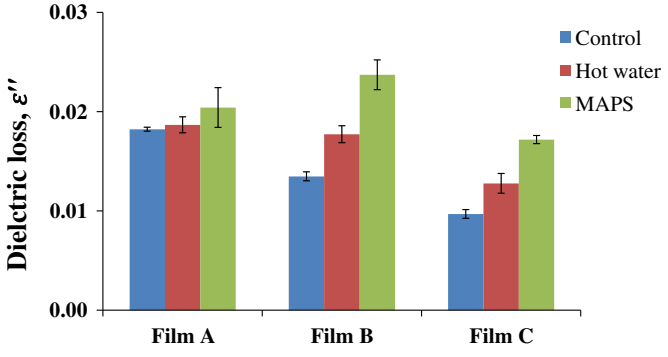

Fig. 8. Dielectric loss of films as influenced by pasteurization processes.

References

ASTM (2010). Standard test method for oxygen gas transmission rate through plastic film and sheeting using a coulometric sensor. *ASTM D3985-05*. Philadelphia, PA: American Society for Testing and Materials.

ASTM (2013). Standard test method for water vapor transmission rate through plastic film and sheeting using a modulated infrared sensor[1]. *ASTM F1249-13*. Philadelphia, PA: American Society for Testing and Materials.

Chen, M., Siochi, E. J., Ward, T. C., & McGrath, J. E. (1993). Basic ideas of microwave processing of polymers. *Polymer Engineering and Science*, *33*(17), 1092–1109.

Clarke, B. (2007). Measurement of dielectric properties of materials at RF and microwave frequencies. In R. J. Collier, & A. D. Skinner (Eds.), *Microwave Measurements* (pp. 409–458). London, UK: The Institute of Engineering and Technology.

Dhawan, S., Varney, C., Barbosa-Canovas, G. V., Tang, J., Selim, F., & Sablani, S. S. (2014a). The impact of microwave-assisted thermal sterilization on the morphology, free volume, and gas barrier properties of multilayer polymeric films. *Journal of Applied Polymer Science*, *131*(12), 40376.

Dhawan, S., Varney, C., Barbosa-Canovas, G. V., Tang, J., Selim, F., & Sablani, S. S. (2014b). Pressure-assisted thermal sterilization effects on gas barrier, morphological, and free volume properties of multilayer EVOH films. *Journal of Food Engineering*, *128*, 40–45.

ECFF, European Chilled Food Federation (2006). Recommendation for the production of prepackaged chilled food. http://www.ecff.net/images/ECFF_Recommendations_2nd_ed_18_12_06.pdf (Accessed September 22, 2016)

Halim, L., Pascall, M. A., Lee, J., & Finnigan, B. (2009). Effect of pasteurization, high-pressure processing, and retorting on the barrier properties of nylon 6, nylon 6/ethylene vinyl alcohol, and nylon 6/nanocomposites films. *Journal of Food Science*, *74*(1), N9–N15.

Kong, Y., & Hay, J. N. (2003). The enthalpy of fusion and degree of crystallinity of polymers as measured by DSC. *European Polymer Journal*, *39*(8), 1721–1727.

Lopez-Rubio, A., Lagaron, J. M., Gimenez, E., Cava, D., Hernandez-Munoz, P., Yamamoto, T., & Gavara, R. (2003). Morphological alterations induced by temperature and humidity in ethylene-vinyl alcohol copolymers. *Macromolecules*, *36*(25), 9467–9476.

López-Rubio, A., Lagarón, J. M., Hernández-Muñoz, P., Almenar, E., Catalá, R., Gavara, R., & Pascall, M. A. (2005). Effect of high pressure treatments on the properties of EVOH-based food packaging materials. *Innovative Food Science & Emerging Technologies*, *6*(1), 51–58.

Mokwena, K. K., Tang, J., Dunne, C. P., Yang, T. C. S., & Chow, E. (2009). Oxygen transmission of multilayer EVOH films after microwave sterilization. *Journal of Food Engineering*, *92*(3), 291–296.

Peng, J., Tang, J., Barrett, D. M., Sablani, S. S., & Powers, J. R. (2014). Kinetics of carrot texture degradation under pasteurization conditions. *Journal of Food Engineering*, *122*, 84–91.

Rabiej, S., OstrowskaGumkowska, B., & Wlochowicz, A. (1997). Investigations of the crystallinity of PA-6/SPS blends by X-ray diffraction and DSC methods. *European Polymer Journal*, *33*(7), 1031–1039.

Reddish, W. (1950). The dielectric properties of polyethylene terephthalate (terylene). *Transactions of the Faraday Society*, *46*, 459–475.

Sammon, C., Yarwood, J., & Everall, N. (2000). An FT-IR study of the effect of hydrolytic degradation on the structure of thin PET films. *Polymer Degradation and Stability*, *67*(1), 149–158.

Solarski, S., Ferreira, M., & Devaux, E. (2005). Characterization of the thermal properties of PLA fibers by modulated differential scanning calorimetry. *Polymer*, *46*, 11187–11192.

TA-211B (2016). Thermal analysis review modultaed DSC therory. *TA instruments*http://www.eng.uc.edu/~beaucag/Classes/Characterization/ModulatedDSC_TAinst.pdf

Tang, J. (2015). Unlocking potentials of microwaves for food safety and quality. *Journal of Food Science*, *80*(8), E1776–E1793.

Verdonck, E., Schaap, K., & Thomas, L. C. (1999). A discussion of the principles and applications of modulated temperature DSC (MTDSC). *International Journal of Pharmaceutics*, *192*(1), 3–20.

Yeh, J. -T., Yao, W. -H., Du, Q., & Chen, C. -C. (2005). Blending and barrier properties of blends of modified polyamide and ethylene vinyl alcohol copolymer. *Journal of Polymer Science Part B: Polymer Physics*, *43*(5), 511–521.

Yoo, S., Lee, J., Holloman, C., & Pascall, M. A. (2009). The effect of high pressure processing on the morphology of polyethylene films tested by differential scanning calorimetry and X-ray diffraction and its influence on the permeability of the polymer. *Journal of Applied Polymer Science*, *112*(1), 107–113.